



Synthesis and Dewatering Properties of Cellulose Derivative-Grafting DMC Amphoteric Biodegradable Flocculants

Xiaodong Chen¹ · Danfeng Wang^{1,2} · Shuang Wang¹ · Hongying Song¹ · Qiang Gu¹ · Yumin Zhang¹

Accepted: 22 September 2020 / Published online: 28 September 2020
© Springer Science+Business Media, LLC, part of Springer Nature 2020

Abstract

Flocculant played an important role in water treatment and sludge dewatering. It is imperative to design and synthesize an eco-friendly and biodegradable flocculant based on natural polymer. In the present work, a new amphoteric CMC-based flocculant, CMC-g-PDMC was synthesized via grafting DMC onto hydroxyl of CMC initiated by potassium persulfate under traditional heating condition. The optimal graft copolymerization condition was optimized by orthogonal experiment. The structure, morphology and thermostability of the obtained graft copolymer were characterized by measuring FT-IR, XRD, SEM and TGA analyzer, respectively. Moreover, comparing with the commercial flocculant PAM, PAC and CPAM, the dewatering capacity of municipal sludge was evaluated using CMC-g-PDMC by FCMC, SRF, SVI and light transmittance. It suggested that the flocculation to municipal sludge was related to the ion properties of the flocculant.

Keywords Cellulose-grafting copolymer · Mechanism · Flocculation · Sludge dewatering · Municipal sludge

Introduction

With the acceleration of industrialization and urbanization, activated sludge produced from industrial and domestic wastewater treatments are giving rise to increasingly serious environmental problems [1, 2]. Because the sludge enriched in insoluble or refractory organic species and heavy metals, it is universally considered to pose serious risks to the ecosystem and human health [3, 4]. Worse still, the moisture content of the sludge is normally higher than 95%. 95% [5, 6], the discharge of sludge containing large volumes of water will take a large number of storage area and waste resources except for increasing the cost for transportation. Besides, sludge is a negatively charged colloid mixture where sludge small particles steadily scattered in water are extremely difficult to be separated from the water phase. Therefore, the sludge dewatering is one of the most challenging subjects in the field of wastewater treatment.

It is known that solid/liquid separation is a central technology in environmental engineering and water treatment. The extensive use of flocculation and settling performance was due to its cost-efficient solid/liquid separation performance [7–9]. It is particularly helpful for separating sludge based on different particle weights [10–15]. What's more, it is of great significance to reduce the volume of sludge for disposal and sludge transport costs.

At present, synthetic flocculants, for example, polyacrylamide and polyacrylic acid, have broadly applied to treatment of industrial wastewater owing to their vast source of raw materials and good flocculation effect [16, 17]. However, these synthesized flocculants are hard to be biodegraded. Also, the harmful monomers produced by their decomposition can even cause potential health hazards [18–22]. Therefore, it is very necessary that the natural biopolymers were synthesized or modified to be eco-friendly flocculants. Cellulose, the most abundant natural organic resource on the earth, has been extensively used as a flocculant for wastewater treatment and sludge dewatering, as it is nontoxic, biodegradable and environmentally friendly [23–26]. Graft copolymerization has been proved to be an effective and convenience modification method for cellulose. Cellulose might react with compounds containing vinyl monomers under mild conditions. This is because there are plenty of hydroxyl groups on cellulose backbone [10, 17, 23–27]. It

✉ Yumin Zhang
zhang_ym@jlu.edu.cn

¹ College of Chemistry, Jilin University, Changchun 130012, People's Republic of China

² Electronic Equipment Research Institute of Sichuan Aerospace, Chengdu 610100, People's Republic of China

is known that sludge colloids are negatively charged. Cationic flocculants can neutralize the negative charge of the sludge colloid well and obtain satisfactory flocculation effect [28, 29]. However, nature polymer-based amphoteric flocculant was rarely applied in sludge dewatering except for chitosan grafting PAA and DMDAAC amphoteric flocculant [30]. This prompted us to explore the synthesis of cellulose based amphoteric flocculants and their applications in sludge dewatering.

In our present work, graft copolymerization between sodium carboxymethyl cellulose (CMC) and methacryloyloxyethyl trimethyl ammonium chloride (DMC) was studied using conventional and convenient free radical polymerization method. The grafted product (CMC-g-PDMC) was expected to possess both cationic and anionic properties, high molecular weight and good solubility, so as to enhance its flocculation. Moreover, the structure, morphology and thermostability of CMC-g-PDMC were characterized by Fourier-transform infrared spectroscopy (FT-IR), X-ray powder diffraction (XRD), scanning electron microscopy (SEM) and thermogravimetric analysis (TGA).

Grafted celluloses were widely applied in wastewater treatment [4, 8], adsorbent of heavy metal ions [31], aggregation of fine kaolin particles [32], etc. However, to the best of our knowledge, no study has been reported that amphoteric CMC-g-PDMC was applied in flocculation and dewatering of the municipal sludge until now. The flocculation and dewatering abilities of CMC-g-PDMC were evaluated by the filter cake moisture content (FCMC), the specific resistance in filtration (SRF), the sludge volume index (SVI) and light transmittance compared with commercially available PAM, cationic polyacrylamide (CPAM), CMC and polyaluminium chloride (PAC). The aim of this work was to prepare a CMC-based flocculant with better flocculation and sludge dewatering capability, inexpensive, biodegradable, and eco-friendly performance.

Material and Methods

Materials

Sodium carboxymethyl cellulose (CMC) with 800–1000 mPa·S viscosity, Methacryloyloxyethyl trimethyl ammonium chloride (DMC) were purchased from Sinopharm Chemical Reagent Co., China. CPAM (cationic degree was 40%), PAM, PAC, acetone and methanol were analytical grade and all purchased from Beijing Chemical Regent Co., China. The above reagents were used directly without further purification. The municipal sludge was obtained from Changchun Nanguan Wastewater Treatment Plant, Jilin, China. The physical properties of the sludge are pH 6.9, the water content 97.2% and SRF 1.83×10^{13} m/kg.

Graft Copolymerization of DMC Onto Cellulose

1 g CMC and the required amount of water were added a four-necked flask to obtain 1.0% concentration aqueous solutions in nitrogen atmosphere. Enough amount of initiator potassium persulfate (KPS) was dropwise added to the above solution. After the solution was heated to the specified temperature, keep stirring for some time. Furthermore, DMC solution was added into the reaction solution. The mixture was continuously stirred at certain temperatures for a while. When the reaction is over, the grafted product was precipitated by adding excess of acetone, and was further filtered. Sequentially, it was respectively washed with ethanol (10 mL \times 3) and water (10 mL \times 3). The homopolymer produced during the reaction was removed by methanol in Soxhlet apparatus. The extractives were dried in a vacuum oven at 60 °C until the weight was constant. The grafting percentage (G) and grafting efficiency (E) of the synthesized CMC-g-PDMC was calculated using the following equation [33]:

$$G = \frac{W_2 - W_0}{W_0} \times 100\%$$

$$E = \frac{W_2 - W_0}{W_1 - W_0} \times 100\%$$

where W_0 and W_2 are the weight of CMC and CMC-g-PDMC, respectively; W_1 is the weight of the crude grafted product (it is not purified by Soxhlet extractor.).

Characterization of CMC-g-PDMC

The grafting polymerization conditions of CMC-g-PDMC were optimized by orthogonal experiment, and the factors and levels are described in Table 1. FT-IR spectra were recorded on a Japan Shimadzu IRAffinity-1 instrument using KBr pellets as a reference in the range between 500 and 4000 cm^{-1} . XRD pattern was measured with a Japan Shimadzu XRD-6100 X-ray diffractometer with graphite monochromatized Cu Ka radiation ($\lambda = 1.54056 \text{ \AA}$). The morphology was collected in a Japan HITACHI SU8020 SEM instrument in powdered form. The TGA curve was

Table 1 Factors and levels of orthogonal experiment

Initiator concentration/ $\times 10^{-3}$ mol/L (A)	Reaction time/h (B)	Reaction temperature/ $^{\circ}\text{C}$ (C)	CMC/DMC mass ratio (D)
2.21	4	65	1:1
3.23	5	70	1:1.5
4.43	6	75	1:2

detected with a USA SDT-Q600 synchronous thermal analyzer under nitrogen atmosphere with a 10 °C/min heating rate from room temperature to 800 °C.

Flocculation Experiments

The dewatering capacity of the municipal sludge was described by calculating FCMC [34], SRF [35], SVI [36] and measuring the light transmittance of filtrate [37]. Dewatering capacity experiment of the sludge was carried out at room temperature, and each experiment was repeated thrice. According to the literature [5], in each test, the pH value of 100 mL sludge was adjusted by dropping 1.0 mol/L HCl or NaOH. Further, the dosage of flocculant was optimized in term of the followed operating conditions: firstly, a rapid stirring of 200 rpm for 30 s, then a slow stirring at 50 rpm for 5 min. After standing 20 min, the conditioned sludge was filtered under a vacuum pressure of 0.05 MPa for 10 min. The dewatering performance and filterability of the sludge was respectively characterized by FCMC, SRF, SVI and light transmittance. The calculated equation of FCMC is as follows [34]:

$$\text{FCMC} = \frac{M_1 - M_2}{M_1} \times 100\%$$

where M_1 and M_2 are respectively the weight of wet filter cake after filtration and the weight of dry filter cake (the wet filter cake was dried to the constant weight at 105 °C.).

SRF was measured by the following equation [35]:

$$\text{SRF} = \frac{2PA^2b}{\mu\omega}$$

where P represents the pressure of filtration (N/m^2); A represents the corresponding filtration area (m^2); μ represents the viscosity of the filtrate ($\text{N}\cdot\text{s/m}^2$); ω is the weight of solids per unit volume of filtrate (kg/m^3); b is the rate of equation in $t/V = bV + a$, t represents the filtration time (s), and V represents the filtrate volume (m^3).

SVI was used to determine the settled sludge volume of a municipal sludge by flocculation after 30 min of the settlement process. It was calculated using the followed equation [36].

$$\text{SVI} = \frac{V}{m_2 - m_0}$$

where V represents the settled sludge volume (mL); m_0 is the weight of a dry culture dish (g); m_2 is the total weight of a dry culture dish and dry filter cake (g). Both the culture dish before the experiment and the wet filter cake were dried to the constant weight at 105 °C.

The filtrated light transmittance was measured using a 723PC UV-spectrophotometer at $\lambda = 650 \text{ nm}$ [37].

Results and Discussion

Graft Copolymerization

It is reported that cellulose-g-PDMC was synthesized using potassium persulfate as an initiator and γ -methacryloxypropyl trimethoxy silane (KH-570) as a coupling agent through a situ grafting copolymerization [32]. In this work, the situ graft copolymerization of CMC and DMC was explored using potassium persulfate as an initiator under conventional heating by the orthogonal experimental method. Because the orthogonal experiment is an efficient approach for rapidly optimizing reaction condition [38, 39]. Normally, in order to obtain the optimal reaction conditions, the experiment of four factors and three levels in each factor will be carried out 3^4 (81) different experiments. Whereas, only 9 experiments were carried out if the orthogonal experiment strategy was adopted. Herein, four investigated factors are initiator concentration, reaction time, reaction temperature, and CMC/DMC mass ratio, and marked as A, B, C and D, respectively. The factors and levels of orthogonal experiment are shown in Table 1. The results of orthogonal experiment and results analysis are summarized in Table 2.

As shown in Table 2, the values of $\sum G_{ij}/3$ and $\sum E_{ij}/3$ represent average value of G and E for three different experiments at each level of a factor, respectively. A high value of $\sum/3$ represents that G or E is high at the level of a factor. Δ represents the difference between the maximum value and minimum value at G or E of a factor. A higher value of ΔG or ΔE illustrates that the effect of the factor on G or E is larger. As shown in Table 2, initiator concentration, reaction time, reaction temperature, and CMC/DMC mass ratio all have a certain effect on the graft copolymerization of CMC and DMC. Also, the influence rule on G and E was consistent. It can be seen from the result analysis (Table 2) that the effect of A on G and E was maximum ($\Delta G = 34.03\%$, $\Delta E = 7.50\%$), was the most primary influencing factor, followed by D ($\Delta G = 10.78\%$, $\Delta E = 5.83\%$) and B ($\Delta G = 9.77\%$, $\Delta E = 3.49\%$), and C ($\Delta G = 5.74\%$, $\Delta E = 1.53\%$) had the weakest influence. The reason was that the active free radicals of monomer were increased with the increase of the concentration of the initiator. As a consequence, the CMC-g-PDMC chain growth rate was accelerated. The molecular weight was increased. However, excessive initiator easily resulted in the implosion both CMC and DMC, the homopolymerization of monomer and chain termination rate was accelerated. It is not helpful to the growth of the chain and the generation of high molecular weight grafted polymer [29]. Consequently, the optimal initiator concentration was $3.23 \times 10^{-3} \text{ mol/L}$. Besides, with the increase of DMC

Table 2 The results of orthogonal experiment and results analysis

Entry	A/mol/L	B/h	C/°C	D	G/%	E/%
1	2.21×10^{-3}	4	65	1:1	43.75	83.33
2	2.21×10^{-3}	5	70	1:1.5	56.25	90.00
3	2.21×10^{-3}	6	75	1:2	45.00	87.80
4	3.23×10^{-3}	4	70	1:2	79.58	95.25
5	3.23×10^{-3}	5	75	1:1	81.25	90.00
6	3.23×10^{-3}	6	65	1:1.5	86.25	89.53
7	4.43×10^{-3}	4	75	1:1.5	80.00	86.15
8	4.43×10^{-3}	5	65	1:2	88.23	86.96
9	4.43×10^{-3}	6	70	1:1	65.16	79.17
$\sum G_{1j/3}$	48.33	67.78	72.74	63.39		
$\sum E_{1j/3}$	87.04	88.24	86.61	84.17		
$\sum G_{2j/3}$	82.36	75.24	67.00	74.17		
$\sum E_{2j/3}$	91.59	88.99	88.14	88.56		
$\sum G_{3j/3}$	77.80	65.47	68.75	70.94		
$\sum E_{3j/3}$	84.09	85.50	87.98	90.00		
ΔG	34.03	9.77	5.74	10.78		
ΔE	7.50	3.49	1.53	5.83		

Table 3 The results of three parallel experiments

Entry	G/%	E/%
1	91.41	96.59
2	92.78	98.43
3	90.67	96.97
$\sum /3$	91.62	97.33

dosage, G and E of graft copolymerization firstly was gradually increased, followed slowly decreased. The possible reason was that excessive DMC caused self-polymerization. Both the graft copolymerization temperature and time were conditioned each other, which was related to the half-life of the initiator. In conclusion, according to the analysis of the experimental results, the optimal synthesis conditions were as follows: The initiator concentration was 3.23×10^{-3} mol/L, the reaction time was 5 h, the reaction temperature was 65–75 °C, CMC/DMC mass ratio was 1:1.5.

To verify the optimal conditions of the graft copolymerization, three parallel experiments were performed (Table 3). The average G and E of three experiments were respectively 91.62% and 97.33%. It suggested that the graft copolymerization between CMC and DMC could be done efficiently under the optimal reaction conditions.

Characterization of CMC-g-PDMC

FT-IR Analysis

FT-IR spectra of CMC (Fig. 1a) and CMC-g-PDMC (Fig. 1b) are shown in Fig. 1. As can be seen from Fig. 1,

both CMC and CMC-g-PDMC have adsorption band around 3440 cm^{-1} , which was attributed to stretching vibration of O–H. This absorption band was broadened in CMC-g-PDMC, which mainly because of the graft copolymerization destroyed part of the hydroxyl in CMC [10, 40]. In FT-IR spectra of CMC (Fig. 1a), the band around 2906 cm^{-1} was attributed to the C–H stretching from the $-\text{CH}_2$ group. The adsorption band at 1607 cm^{-1} was attributed to the antisymmetrical stretching vibration of carboxylate COO^- [41]. The characteristic absorption of β -(1,4) glycoside bond of cellulose can be observed around 1039 cm^{-1} . In FT-IR spectra of CMC-g-PDMC (Fig. 1b), the new adsorption peak appeared at 3016 cm^{-1} and 2932 cm^{-1} were the antisymmetrical stretching vibration of $-\text{CH}_3$ and $-\text{CH}_2$ group on quaternary ammonium nitrogen, respectively. The new adsorption peak appeared at 1730 cm^{-1} and 1265 cm^{-1} were ascribed to the stretching vibration of C=O on ester group and C–C(=O)–O of DMC, respectively. The new peak presented at 1481 cm^{-1} was attributed to the bending vibration peaks of $-\text{CH}_2-\text{N}^+(\text{CH}_3)_3$ group of DMC [5, 42]. The new peak at 954 cm^{-1} was the characteristic absorption peak of quaternary ammonium nitrogen [43]. Besides, the adsorption peak at 1607 cm^{-1} of carboxylate COO^- (Fig. 1a) was blue-shifted to 1604 cm^{-1} (Fig. 1b). It can be confirmed from Fig. 1 analysis that DMC had been grafted onto the backbone of the cellulose.

XRD Analysis

XRD pattern of CMC-g-PDMC shows distinct crystalline peaks compared with that of CMC (Fig. 2). The pattern of CMC displayed two peaks around $2\theta = 20^\circ$ and $2\theta = 37^\circ$,

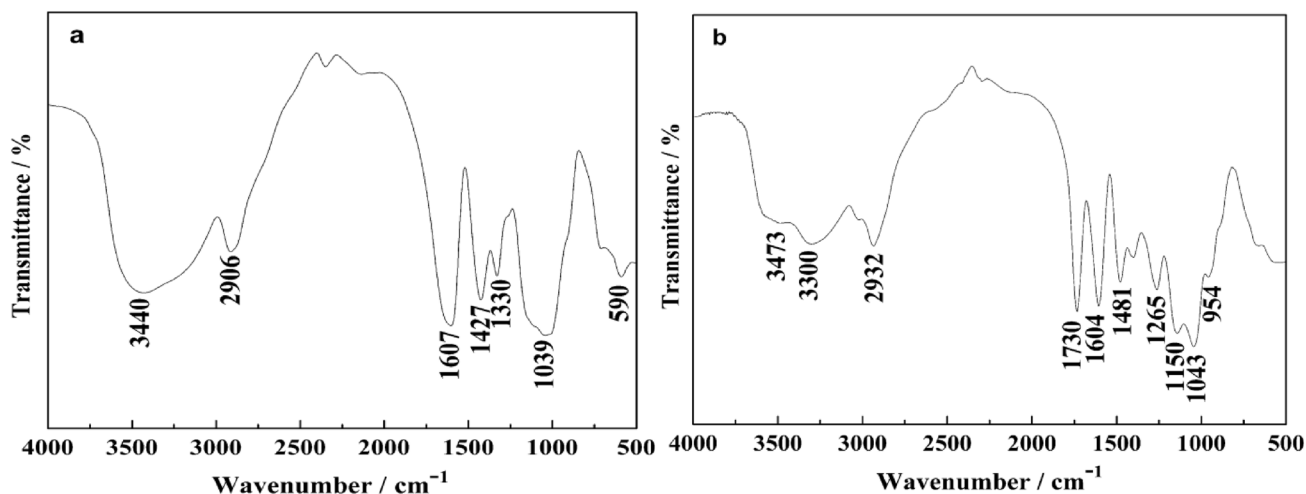


Fig. 1 FT-IR spectra of CMC (a) and CMC-g-PDMC (b)

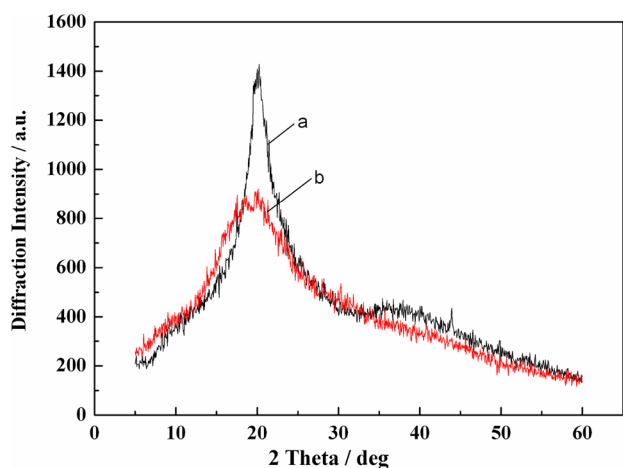


Fig. 2 XRD of CMC (a) and the CMC-g-PDMC (b)

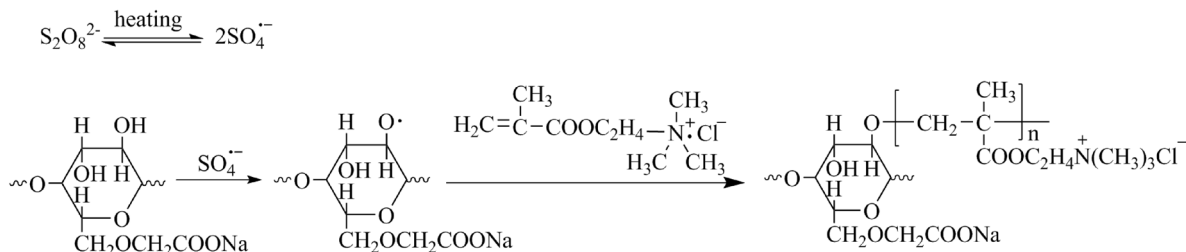
which was according to the CMC characteristic X-ray diffraction pattern reported by the literature [44]. However, in XRD profiles of CMC-g-PDMC, the peak at $2\theta = 20^\circ$ decreased sharply, and the peak at $2\theta = 37^\circ$ disappeared.

The decrease in crystallinity of CMC-g-PDMC suggested that the hydrogen bond interactions CMC possessed were weakened. This resulted from $-\text{OH}$ on CMC had carried out the graft copolymerization with DMC [28].

According to the analysis results of IR spectrum and XRD pattern of CMC-g-PDMC, the possible graft copolymerization mechanism of CMC and DMC is concluded in Scheme 1. The reaction process was consistent with the view which the sulfate radicals can react with hydroxyl group of the compounds [45, 46]. Herein, the dissociated $\text{S}_2\text{O}_8^{2-}$ from potassium persulfate in water was dissolved into sulfate radicals $\text{SO}_4^{\cdot-}$ by heating. Further, sulfate radicals captured hydrogen from hydroxyl group on CMC and generate CMC macro radicals. The obtained macromolecular radicals rapidly reacted with DMC monomer and initiated graft copolymerization.

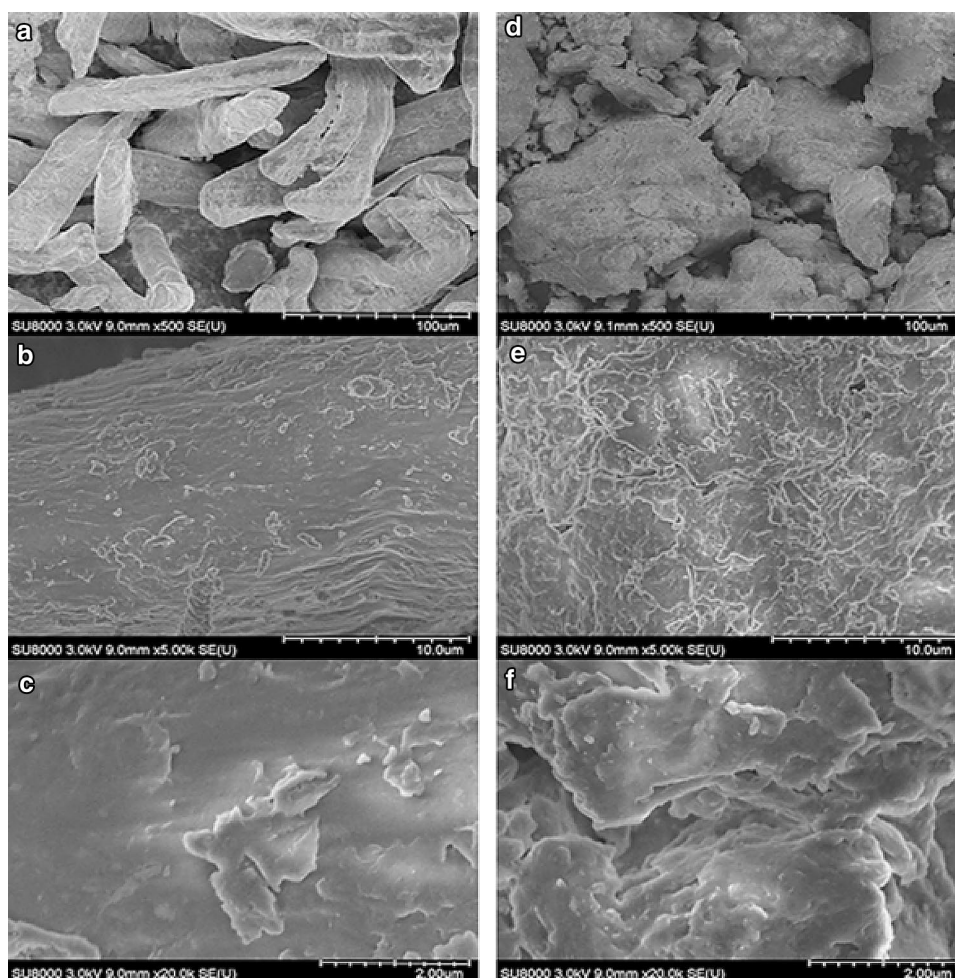
SEM Analysis

As shown in Fig. 3, SEM micrographs of CMC (Fig. 3a–c) and CMC-g-PDMC (Fig. 3d–f) displayed significant morphological change. After DMC was grafted onto CMC, the



Scheme 1 The possible graft copolymerized mechanism of CMC and DMC

Fig. 3 SEM of CMC (a, b, c) and the CMC-g-PDMC (d, e, f)



morphology has changed from smooth round bar surface (CMC) to an irregular block lamellar structure (CMC-g-PDMC) with many honeycomb or scaly, which improved specific surface area of CMC. The high specific surface area might enhance the adsorption ability and bridging effect of the flocculant because it might increase the contact probability between the synthesized CMC-g-PDMC (flocculant) and sludge [47, 48].

Thermogravimetric Analysis

Figure 4 shows the thermal behavior differences between CMC and CMC-g-PDMC. CMC displayed two weight losses (Fig. 4a). The first weight loss was between 50 and 170 °C, which might be due to the loss of surface absorbed and bound water. The second stage of weight loss occurred at 260–310 °C, which was possibly ascribed to the thermal decomposition of CMC backbone. Also, the thermal decomposition temperature of CMC was 262 °C. Compared with CMC, TGA curve of CMC-g-PDMC (Fig. 4b) showed three stages of weight losses. The weight loss at 50–170 °C was more than that of CMC. This was because the weight

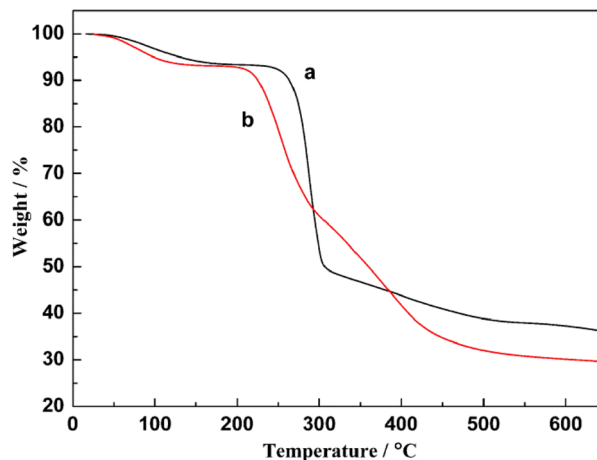


Fig. 4 TGA of CMC (a) and CMC-g-PDMC (b)

losses also related with the adsorbed quaternary ammonium salt DMC decomposition except for relating with the loss of surface absorbed and bound water. Besides, the other two stages of weight loss were respectively at 210–300 °C and

300–420 °C. The weight loss at 210–300 °C also was due to the thermal decomposition of CMC backbone. The weight losses at 300–420 °C might be assigned to the formation of Na_2CO_3 [49] and the corresponding loss of ammonia and water by imidization and dehydration [50]. The thermal decomposition temperature of CMC-g-PDMC was 221 °C. It indicated that DMC had been grafted onto CMC, and the thermal stability of CMC-g-PDMC was just below that of CMC.

Sludge Dewatering Performance

Effect of the Dosage on the Sludge Dewatering Efficiency

Figure 5 shows the effect of flocculant CMC, CMC-g-PDMC, PAM and CPAM dosage on FCMC. FCMC may directly reflect the degree of difficulty for sludge dewatering. Four flocculants all exhibited the different trend. Adding the flocculant PAM and CMC-g-PDMC, FCMC initially decreased rapidly, decreased slowly, then, increased slowly. Correspondingly, adding the flocculant CMC and CPAM, FCMC decreased rapidly, then increased slowly, which is because the flocculation mainly derived from bridging adsorption at the added lower dosage. Furthermore, achieving the best flocculation effect need to add the different dosage flocculants that CMC was 15 mg/L (FCMC 76.46%), CMC-g-PDMC was 25 mg/L (FCMC 72.01%), PAM was 30 mg/L (FCMC 76.06%) and CPAM was 20 mg/L (FCMC 70.08%). Therefore, the dewatering efficiency of CPAM was the best, followed by CMC-g-PDMC and then CMC and PAM. This might be because CPAM with cation and CMC-g-PDMC with both cation and an irregular block lamellar structure were helpful to improve the bridging adsorption and charge-neutralizing ability to promote sludge dewatering

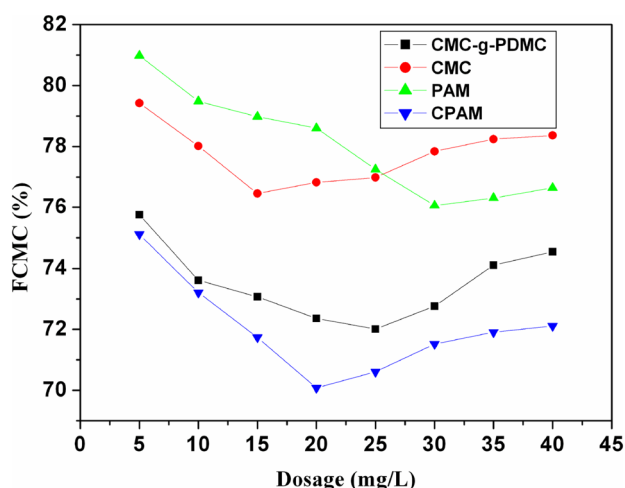


Fig. 5 Effect of CMC, CMC-g-PDMC, CPAM and PAM dosages on FCMC with pH at 6.9

[51]. However, the flocculation was decreased when excess CPAM and CMC-g-PDMC were used in sludge dewatering. This resulted from extra positive charge on CPAM or extra positive charge along with negative charge on CMC-g-PDMC regenerating the repulsion forces to result in sludge instability. But, CMC and PAM showed the bad effects of sludge dewatering, because they have not cations that can neutralize the negative charge of sludge colloids. However, the dewatering efficiency of CMC was superior to PAM because of plenty of hydroxyl group on the backbone of CMC might adsorb negative charge.

Effect of pH on Dewatering Performance

It is reported that acid and alkali had a great influence on sludge dewatering of the flocculant [52]. The effect of pH on FCMC by adding CMC and CMC-g-PDMC are shown in Fig. 6. Where the flocculation of CMC and CMC-g-PDMC presented similar change profiles, and their sludge dewatering effects were gradually decreased in turn adding CMC-g-PDMC and CMC at the same pH. It mainly was ascribed to cationic charge neutralization. Their FCMC decreased slowly when pH adjusted from 2.0 to 4.0 and respectively obtained minimum 71.29% (CMC-g-PDMC) and 75.00% (CMC) at pH 4, then FCMC increased slowly, followed by being increased rapidly when pH increased from 4.0 to 8.0 and from 8.0 to 10.0. When pH was at 4.0–7.0, the FCMC was 71.00–74.00% after the sludge was dewatered through the flocculation of CMC-g-PDMC. It indicated that CMC-g-PDMC had good flocculation and dewatering performance at 3.0–7.0. At $\text{pH} < 3$, excessive hydrogen ions repulsed the positive charges of amphoteric polymer CMC-g-PDMC, which led to the negatively charged sludge colloids being difficult to settle. However, in the presence of alkali, the

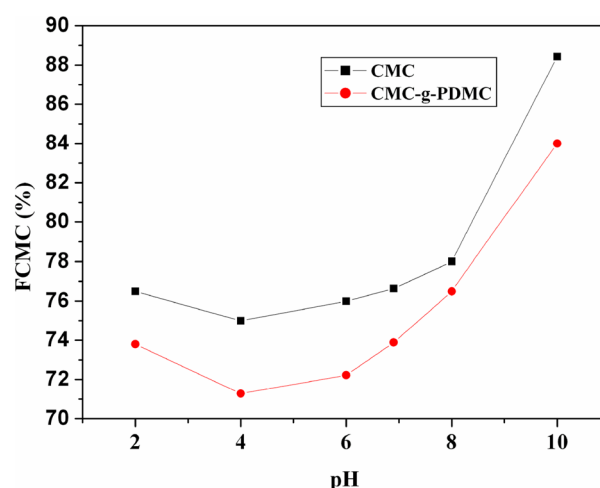


Fig. 6 Effect of pH on FCMC for CMC and CMC-g-PDMC at dosage of 25 mg/L

positive charges of DMC grafted onto CMC chains took preference to neutralized with hydroxyl ion, which decreased the charge neutralization ability to negative charge on a colloidal particle of sludge. Especially, At $\text{pH} > 8$, the sludge dewatering became more difficult, and FCMC rapidly increased to close to FCMC for the municipal sludge dewatered in the absence of the flocculant, which lied in the fact that re-dispersion resulted from charge reversion except for the competition of charge neutralization and bridging adsorption [53, 54].

Effect of Temperature on Dewatering Performance

Figure 7 shows the effect of the temperature on sludge dewatering (pH 6.9) of CMC and CMC-g-PDMC. The FCMC using CMC and CMC-g-PDMC as flocculants both decreased gradually in terms of temperature increase, and CMC-g-PDMC displayed superior sludge dewatering performance over CMC. The main reason might lie in the fact that the high temperature can accelerate not only the movement and aggregation of sludge colloid particles but also the dissolution and movement of CMC and CMC-g-PDMC to enhanced bridging adsorption. Therefore, it is helpful to sludge dewatering by the temperature enhanced.

Effect of Different Grafting Percentage CMC-g-PDMC on Dewatering Performance

Figure 8 shows the effect of different grafting percentage CMC-g-PDMC on FCMC. FCMC decreased linearly, followed by rapidly increased, and then increased slowly with grafting percentage increase at 25 mg/L dosage, pH at 6.9, temperature at 25 °C, grafting percentage in 43.75–88.23%.

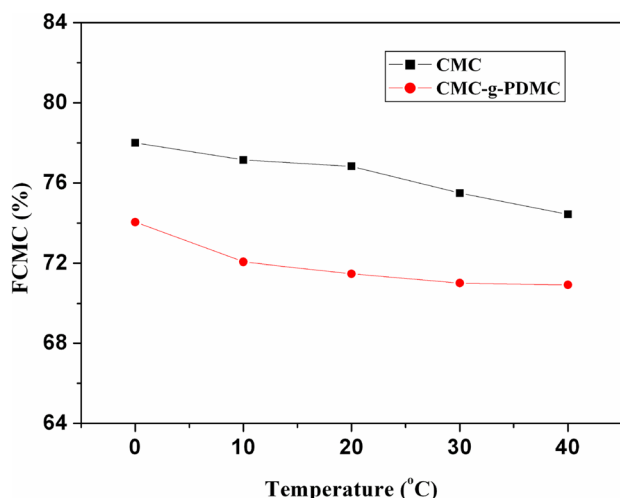


Fig. 7 Effect of temperature on FCMC for CMC and CMC-g-PDMC with dosage at 25 mg/L

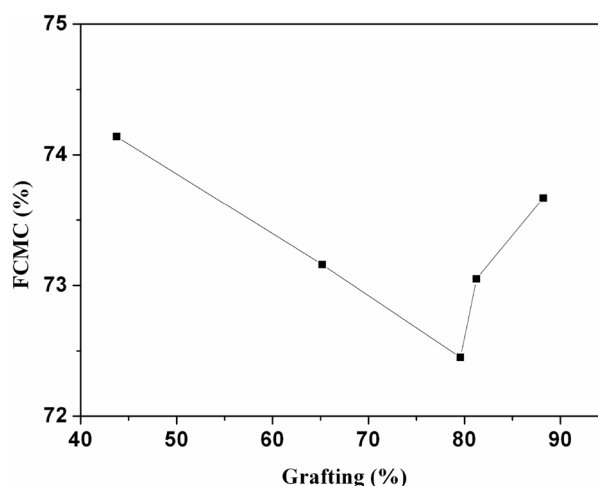


Fig. 8 Effect of different grafting percentage CMC-g-PDMC on FCMC

It is seen from Fig. 8 that the flocculation performance of CMC-g-PDMC was the best (FCMC: 72.45%) when the grafting percentage was around 80%. Under the relatively low grafting percentage conditions (43.75–80.00%), the decrease of FCMC mainly derived from the ability of charge neutralization and bridging of CMC-g-PDMC. However, when the grafting percentage exceeded to 80%, the FCMC was gradually increased, which resulted from part of positive charge unable to do neutralization very well owing to the steric and electrostatic repulsion. As a result, it might lead to uneven distribution of charge on the sludge colloid and instability, further influenced the effect of sludge dewatering.

Comparison of the Dewaterability of the Municipal Sludge by SRF

To investigate the flocculation and dewatering capacity of the municipal sludge by adding the different flocculants PAM, CPAM, and CMC-g-PDMC, the effects of the dosage of the flocculant on SRF were measured under pH at 6.9 and room temperature conditions (Fig. 9). It can be seen from Fig. 9 that SRF of the sludge using PAM as a flocculant was the highest among PAM, CPAM, and CMC-g-PDMC, followed by the amphoteric flocculant CMC-g-PDMC, the lowest SRF which was due to the introduction of the cation flocculant CPAM. This was because PAM, CMC-g-PDMC and CPAM respectively had no ions, both cations and anions, cations, respectively. Therefore, their charge neutralization ability was $\text{CPAM} > \text{CMC-g-PDMC} > \text{PAM}$. Also, it can be seen from the flocs obtained after flocculation by the above three flocculants, the flocs are large and dense by CPAM, followed by CMC-g-PDMC, finely dispersed by PAM, respectively. That is to say, charge neutralization could reduce the thickness of the hydrated shell of the particles surface and

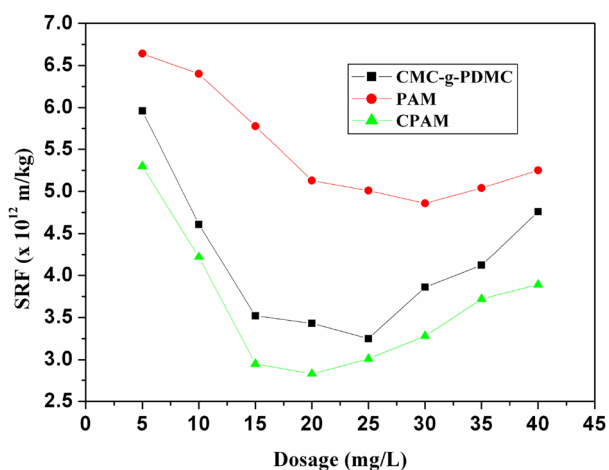


Fig. 9 Effect of CMC-g-PDMC, CPAM and PAM dosages on SRF

improve the flow of free water due to decreasing the surface tension of water and compressing the thickness of the electric double layer [29]. In consequence, the lowest SRF was respectively 2.83×10^{12} m/kg and 3.01×10^{12} m/kg (CPAM, 20 mg/L and 25 mg/L), 3.25×10^{12} m/kg (CMC-g-PDMC, 25 mg/L) and 4.86×10^{12} m/kg (PAM, 30 mg/L). The sludge after flocculation by the above flocculants was easily dewatered according to the reported literature [55] (it had been reported in the literature [55] that the sludge with $\text{SRF} > 1.00 \times 10^{13}$ m/kg and $\text{SRF} < 4.00 \times 10^{12}$ m/kg was respectively attributed to difficult or easy dewatered sludge.). In addition, SRF of the sludge using polyaluminium chloride (PAC) as a flocculant with the dosage change was also investigated. The lowest SRF was 4.57×10^{12} m/kg when the added PAC dosage was 2.0 g/L (because the added PAC dosage was too high to present in Fig. 9). It indicated that the sludge dewatering performance of PAC was comparatively low. Besides, SRF of the sludge after flocculation by three flocculants all initially decreased rapidly, leveled off, then, increased slowly with the dosage increase. These change laws is consistent with that of Fig. 5.

Comparison of the Settling Performance of the Municipal Sludge by SVI and the light transmittance

It was reported that SVI value was influenced by osmotic pressure, hydration force and flocculation effect [36, 56]. SVI is an indicator of sludge settling performance. The smaller SVI was, the better the sludge settling performance was. Figure 10 shows the effect of flocculant CMC-g-PDMC, PAM and CPAM dosage on SVI. It is seen from Fig. 10 that the flocculant CPAM and CMC-g-PDMC presented good flocculation comparing with

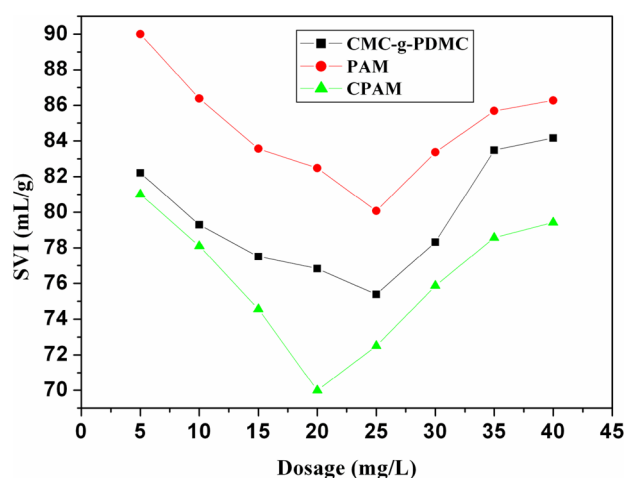


Fig. 10 Effect of CMC-g-PDMC, CPAM and PAM dosages on SVI

PAM. Also, SVI of three samples shows the same change trend with the dosage increase, The lowest SVI value was respectively 80.07 mL/g (25 mg/L, PAM), 75.38 mL/g (25 mg/L, CMC-g-PDMC) and 70.00 mL/g (20 mg/L, CPAM (25 mg/L, 72.50 mL/g)). This is because the charge neutralization of the cations with the negative charge on the sludge colloid resulted in the gap region between two particle surfaces to be reduced, further caused the osmotic pressure and hydration force to be decreased, consequently decreased the range of repulsive force and considerably, aggregated the sludge flocs and released their bonding water molecules. SVI by CMC-g-PDMC flocculation was lower than that of CPAM, which was attributed to the DMC and COO^- on CMC-g-PDMC chain acted together on the sludge colloid. SVI by PAM flocculation was high due to no cations on PAM chain.

Besides, the filtrate transmittance of the sludge was also used to evaluate the flocculation effect. The light transmittance was high indicated the sludge particle well accumulated. The effects of flocculant CMC-g-PDMC, PAM and CPAM dosage on the light transmittance are presented in Fig. 11. At the optimal dosage of the flocculant, their highest light transmittance was respectively 91.67% (CMC-g-PDMC), 90.20% (PAM) and 92.60% (CPAM). In addition, the filtrate transmittance of the sludge by the dosage of PAC flocculation was also measured, its highest light transmittance was 90% (2 g/L). Compared to the filtrate transmittance of the untreated sludge (80%), the filtrate transmittance of the sludge was obviously improved. To sum up, the sludge dewatering effect by the cationic flocculant CPAM was the best one, followed by amphoteric flocculant CMC-g-PDMC, then non-ionic flocculant PAM and inorganic flocculant PAC.

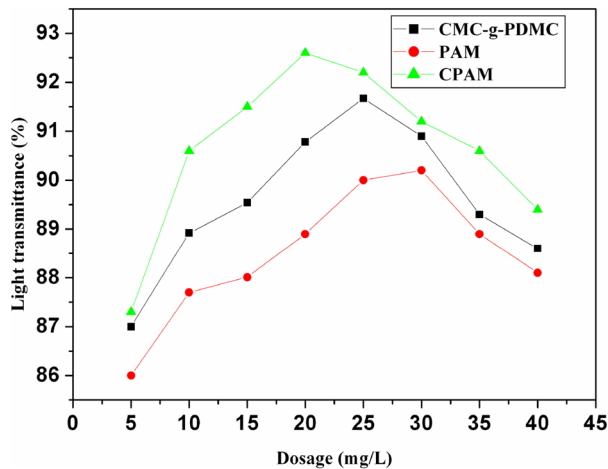


Fig. 11 Effect of CMC-g-PDMC, CPAM and PAM dosages on light transmittance

Conclusions

A convenient and cost-efficient method for synthesizing CMC-g-PDMC flocculant starting from CMC and DMC was developed. A new eco-friendly and biodegradable flocculant was prepared. The optimal graft copolymerization condition was determined by orthogonal experiment. The reaction mechanism was deduced. It proved that DMC had been grafted onto CMC by analysing its IR spectra, XRD and SEM pattern, and the thermal behavior. Further, the sludge dewaterability was studied comparing with the flocculation of CMC, PAM, CPAM and PAC by FCMC, SRF, SVI and the filtrate transmittance. The experimental results indicated that the optimal flocculation conditions using CMC-g-PDMC to flocculate the municipal sludge were the dosage of 25 mg/L, pH at 3–7, the higher temperature was helpful to flocculation, and the grafting percentage was around 80%. FCMC, SRF, SVI and the filtrate transmittance by CMC-g-PDMC flocculation were respectively 72.01%, 3.25×10^{12} m/kg, 75.38 mL/g and 91.67%. The sludge dewatering capacity was also demonstrated to be better than that of PAC, PAM, CMC, lower than that of CPAM. The above results revealed that CMC-g-PDMC as a nontoxic, environmentally friendly and biodegradable flocculant possess the potential applications in the sludge dewatering and wastewater treatment. Moreover, the synthesis of other nature graft copolymer and the application in sludge dewatering are in process in our laboratory.

Acknowledgements The research was supported by Beijing Guoneng Zhongtian Environmental Protection Technology Co. Ltd. of China and the key project of Science and Technology Department of Jilin province of China (Project No.20090416).

References

1. Lv S, Sun T, Zhou Q, Liu J, Ding H (2014) Synthesis of starch-g-p(DMDAAC) using HRP initiation and the correlation of its structure and sludge dewaterability. *Carbohydr Polym* 103:285–293
2. Atangana E, Oberholster PJ (2020) Modified biopolymer (chitin-chitosan derivatives) for the removal of heavy metals in poultry wastewater. *J Polym Environ* 28:388–398
3. Chai L, Li H, Yang Z, Min X, Liao Q, Liu Y, Men S, Yan Y, Xu J (2017) Heavy metals and metalloids in the surface sediments of the Xiangjiang River, Hunan, China: distribution, contamination, and ecological risk assessment. *Environ Sci Pollut Res* 24:874–885
4. Meena RAA, Sathishkumar P, Ameen F, Yusoff ARM, Gu F (2018) Heavy metal pollution in immobile and mobile components of lentic ecosystems—a review. *Environ Sci Pollut Res* 25:4134–4148
5. Zheng HL, Sun YJ, Guo JS, Li FT, Fan W, Liao Y, Guan QQ (2014) Characterization and evaluation of dewatering properties of PADB, a highly efficient cationic flocculant. *Ind Eng Chem Res* 53:2572–2582
6. Qi Y, Thapa KB, Hoadley AFA (2011) Application of filtration aids for improving sludge dewatering properties—a review. *Chem Eng J* 171:373–384
7. Lapointe M, Barbeau B (2020) Understanding the roles and characterizing the intrinsic properties of synthetic vs. natural polymers to improve clarification through interparticle Bridging: a review. *Sep Purif Technol* 231:115893
8. Sillanpää M, Ncibi MC, Matilainen A, Vepsäläinen M (2018) Removal of natural organic matter in drinking water treatment by coagulation: a comprehensive review. *Chemosphere* 190:54–71
9. Yang R, Li H, Huang M, Yang H, Li A (2016) A review on chitosan-based flocculants and their applications in water treatment. *Water Res* 95:59–89
10. Wang Zh, Huang W, Yang G, Liu Y, Liu S (2019) Preparation of cellulose-base amphoteric flocculant and its application in the treatment of wastewater. *Carbohydr Polym* 215:179–188
11. Harif T, Adin A (2007) Characteristics of aggregates formed by electroflocculation of a colloidal suspension. *Water Res* 41(2951–2961):1
12. Pourrezaei P, Drzewicz P, Wang YN, El-Din MG, Perez-Estrada LA, Martin JW, Anderson J, Wiseman S, Liber K, Giesy JP (2011) The impact of metallic coagulants on the removal of organic compounds from oil sands process affected water. *Environ Sci Technol* 45:8452–8459
13. Yang Z, Yuan B, Huang X, Zhou JY, Cai J, Yang H, Li AM, Cheng RS (2012) Evaluation of the flocculation performance of carboxymethyl chitosan-graft-polyacrylamide, a novel amphoteric chemically bonded composite flocculant. *Water Res* 46:107–114
14. Yang Q, Luo K, Liao DX, Li XM, Wang DB, Liu X, Zeng GM, Li X (2012) A novel bioflocculant produced by *Klebsiella* sp. and its application to sludge dewatering. *Water Environ J* 26:560–566
15. Besra L, Sengupta DK, Roy SK, Ay P (2004) Influence of polymer adsorption and conformation on flocculation and dewatering of kaolin suspension. *Sep Purif Technol* 37:231–246
16. Pal S, Ghorai S, Dash MK, Ghosh S, Udayabhanu G (2011) Flocculation properties of polyacrylamide grafted carboxymethyl guar gum (CMG-g-PAM) synthesised by conventional and microwave assisted method. *J Hazard Mater* 192:1580–1588
17. Zhu H, Zhang Y, Yang X, Shao L, Zhang X, Yao J (2016) Polyacrylamide grafted cellulose as an eco-friendly flocculant: key factors optimization of flocculation to surfactant effluent. *Carbohydr Polym* 135:145–152
18. Bo XW, Gao BY, Peng N, Wang Y, Yue QY, Zhao YC (2012) Effect of dosing sequence and solution pH on floc properties of the

- compound bioflocculant-aluminum sulfate dual-coagulant in kaolin-humic acid solution treatment. *Bioresour Technol* 113:89–96
19. Song Y, Zhang J, Gan W, Zhou J, Zhang L (2010) Flocculation properties and antimicrobial activities of quaternized celluloses synthesized in NaOH/Urea aqueous solution. *Ind Eng Chem Res* 49:1242–1246
 20. Moreno-Chulim MV, Barahona-Perez F, Canche-Escamilla G (2003) Biodegradation of starch and acrylic-grafted starch by *Aspergillus niger*. *J Appl Polym Sci* 89:2764–2770
 21. Xing W, Ngo HH, Guo WS, Wu ZQ, Nguyen TT, Cullum P, Lisowski A, Yang N (2010) Enhancement of the performance of anaerobic fluidized bed bioreactors (AFBBRs) by a new starch based flocculant. *Sep Purif Technol* 72:140–146
 22. Bratskaya S, Schwarz S, Chervonetsky D (2004) Comparative study of humic acids flocculation with chitosan hydrochloride and chitosan glutamate. *Water Res* 38:2955–2961
 23. Yan L, Tao H, Bangal P (2009) Synthesis and flocculation behaviour of cationic cellulose prepared in a NaOH/urea aqueous solution. *Clean (Weinh)* 37:39–44
 24. Ahlgren J (2014) Future biorefineries: Products from dissolved cellulose program report fibic, Forestcluster Ltd, pp 102–121
 25. Ott G, Schempp W, Krause T (1989) Preparation of cationic cellulose with high degree of substitution in lithium chloride/dimethylacetamide. *Papier* 43:694–699
 26. Moser T, Schmalhofer A, Spedding J, Oberkofler J (1996) Cationic cellulose particles for flocculation or retention agents for papermaking. *Ger Offen DE 19520804(A1)*:19960822
 27. Sen G, Mishra S, Rani GU, Prasad R (2012) Microwave initiated synthesis of polyacrylamide grafted Psyllium and its application as a flocculant. *Int J Biol Macromol* 50(2):369–375
 28. Wang JP, Yuan SJ, Wang Y, Yu HQ (2013) Synthesis, characterization, and application of a novel starch based flocculant with high flocculation and dewatering properties. *Water Res* 47:2643–2648
 29. Wang D, Zhao T, Yan L, Mi Zh, Gu Q, Zhang Y (2016) Synthesis, characterization and evaluation of dewatering properties of chitosan-grafting DMDAAC flocculants. *Int J Biol Macromol* 92:761–768
 30. Fan J, Chen Q, Li J, Wang D, Zheng R, Gu Q, Zhang Y (2019) Preparation and dewatering property of two sludge conditioners chitosan/AM/AA and chitosan/AM/AA /DMDAAC. *J Polym Environ* 27:275–285
 31. Chai L, Li Q, Wang Q, Yan X (2018) Solid-liquid separation: an emerging issue in heavy metal wastewater treatment. *Environ Sci Pollut Res* 25:17250–17267
 32. Li M, Wang Y, Hou X, Wan X, Xiao H-N (2018) DMC-grafted cellulose as green-based flocculants for agglomerating fine kaolin particles. *Green Energy Environ* 3:138–146
 33. Wan Sh, Hao H, Shao Z (2004) Studies on preparation of amphoteric cellulose from nature plant straw. *Polym Mater Sci Eng (China)* 20(5):190–193
 34. Liao Y, Zheng H, Qian L, Sun Y, Dai L, Xue W (2014) UV-Initiated polymerization of hydrophobically associating cationic polyacrylamide modified by a surface-active monomer: a comparative study of synthesis, characterization, and sludge dewatering performance. *J Ind Eng Chem Res* 53:11193–11203
 35. Lin Q, Peng H, Zhong S, Xiang J (2015) Synthesis, characterization, and secondary sludge dewatering performance of a novel combined silicon-aluminum-iron-starch flocculant. *J Hazard Mater* 285:199–206
 36. Mohtar SS, Busu TN, Noor AM, Shaari N, Yusoff NA, Yunus MA, Mat H (2017) Optimization of coag-flocculation processes of a newly synthesized quaternized oil palm empty fruit bunch cellulose by response surface methodology toward drinking water treatment process application. *Clean Technol Environ Policy* 19:191–204
 37. Qin M, Zhao H, Li R, Wang Zh (2014) Coagulation efficiency of covalent bonded aluminum-silicon hybrid flocculants. *Chin J Environ Eng* 8(4):1262–1266
 38. Lu YB, Shang YB, Huang X, Chen AM, Yang Zh, Jiang Y, Cai J, Gu W, Qian X, Yang H, Cheng R (2011) Preparation of strong cationic chitosan-graft-polyacrylamide flocculants and their flocculating properties. *Ind Eng Chem Res* 50:7141–7149
 39. Ge HC, Pang W, Luo DK (2006) Graft copolymerization of chitosan with acrylic acid under microwave irradiation and its water absorbency. *Carbohydr Polym* 66:372–378
 40. Kurenkov F, Shatokhina V, Hartan G, Lobanov I (2005) Sedimentation of kaolin suspension in the presence of praestol anionic flocculant and aluminum polyoxochloride and sulfate coagulants. *Russ J Appl Chem* 78:1872–1875
 41. Zhang H, Peng QJ, Li YM, Zhang R (2005) Modern organic spectroscopy. Chemical industry Press, Beijing, p 261
 42. Nourani M, Baghdadi M, Javan M, Bidhendi N (2016) Production of a biodegradable flocculant from cotton and evaluation of its performance in coagulation/flocculation of kaolin clay suspension: optimization through response surface methodology (RSM). *J Environ Chem Eng* 4:1996–2003
 43. Cai T, HJ Li, Yang R, Wang YW, Li RH, Yang H, Li A, Cheng RS (2015) Efficient flocculation of an anionic dye from aqueous solutions using a cellulose-based flocculant. *Cellulose* 22:1439–1449
 44. Kuila SB, Ray SK (2014) Separation of benzene-cyclohexane mixtures by filled blend membranes of carboxymethyl cellulose and sodium alginate. *Sep Purif Technol* 123:45–52
 45. Mukhopadhyay S, Prasad J, Chatterjee SR (1975) Grafting of acrylic acid onto methylcellulose. *Die Makromol Chem* 176:1–7
 46. Panesar SS, Jacob S, Misra M, Mohanty AK (2013) Functionalization of lignin: fundamental studies on aqueous graft copolymerization with vinyl acetate. *Ind Crops Prod* 46:191–196
 47. Li X, Zheng H, Gao B, Zhao C, Sun Y (2017) UV-initiated polymerization of acid and alkali-resistant cationic flocculant P(AM-MAPTAC): synthesis, characterization, and application in sludge dewatering. *Sep Purif Technol* 187:244–254
 48. Thapa KB, Qi Y, Clayton SA, Hoadley AFA (2009) Lignite aided dewatering of digested sewage sludge. *Water Res* 43:623–634
 49. Kalagasidis Krušić M, Džunuzović E, Trifunović SS, Filipović J (2004) Polyacrylamide and poly(itaconic acid) complexes. *Eur Polym J* 40:793–798
 50. Van Dyke JD, Kasperski KL (1993) Thermogravimetric study of polyacrylamide with evolved gas analysis. *J Polym Sci A* 31:1807–1823
 51. Yang Z, Yang H, Jiang Z, Cai T, Li H, Li A, Cheng R (2013) Flocculation of both anionic and cationic dyes in aqueous solutions by the amphoteric grafting flocculant carboxymethyl chitosan-graft-polyacrylamide. *J Hazard Mater* 254–255:36–45
 52. Raynaud M, Vaxelaire J, Olivier J, Fauvel ED, Baudez JC (2012) Compression dewatering of municipal activated sludge: effects of salt and pH. *Water Res* 46:4448–4456
 53. Sarkar AK, Mandre NR, Panda AB, Pal S (2013) Amylopectin grafted with poly (acrylic acid): development and application of a high performance flocculant. *Carbohydr Polym* 95:753–759
 54. Sharma BR, Dhuldhoya NC, Merchant UC (2006) Flocculants-an ecofriendly approach. *J Polym Environ* 14:195–202
 55. Liang HJ, Shi L, Yang GY (2014) Improving sludge dewaterability by adding the semi-dry flue gas desulfurization residue under microwave radiation. *Clean: Soil, Air, Water* 42(9999):1–9
 56. Ives KJ, Al Dibouni M (1979) Orthokinetic flocculation of latex microspheres. *Chem Eng Sci* 34:983–991